



The structural catalyst $\text{CuMoO}_4/\text{TiO}_2/\text{TiO}_2 + \text{SiO}_2/\text{Ti}$ for diesel soot combustion

N.V. Lebukhova^{a,1}, V.S. Rudnev^{b,c,2}, E.A. Kirichenko^{a,3}, P.G. Chigrin^{a,*,4}, I.V. Lukiyanichuk^{b,5}, N.F. Karpovich^{a,6}, M.A. Pugachevsky^{a,7}, V.G. Kurjavij^{b,8}

^a Institute of Materials of Khabarovsk Scientific Centre, Far Eastern Branch of the Russian Academy of Sciences, 153, Tikhookeanskaya Street, Khabarovsk 680042, Russia

^b Institute of Chemistry, Far Eastern Branch, Russian Academy of Sciences, 159, Prosp. 100-letya Vladivostoka, Vladivostok 690022, Russia

^c Far Eastern Federal University, 8, Sukhanova Street, Vladivostok 690950, Russia

ARTICLE INFO

Article history:

Received 31 July 2014

Accepted in revised form 1 November 2014

Available online 8 November 2014

Keywords:

Ti support

Catalytic coating

Adherence

Diesel soot oxidation

ABSTRACT

A Ti surface treated by plasma electrolytic oxidation (PEO) in silicate electrolyte has been coated with the nanostructural TiO_2 layer and then impregnated using the sol–gel method with Cu and Mo, which are active ingredients for soot combustion. The layer TiO_2 consists of anatase crystals of up to 50 nm, and has a mosaic-like structure with interconnected surface cracks. The quantity and volume of microcracks depend on both a concentration of the TiO_2 colloidal suspension and a regime of its heat treatment. After impregnation with Cu and Mo and calcination at 550 °C, the surface of the TiO_2 layer is evenly covered by the CuMoO_4 particles of 150–350 nm. The catalytic performance for diesel soot combustion was analyzed under loose contact conditions of soot and catalyst. The structured catalysts $\text{CuMoO}_4/\text{TiO}_2/\text{TiO}_2 + \text{SiO}_2/\text{Ti}$ provide diesel soot combustion above 280 °C with two maximum rates of 340–360 °C (soot combustion in volume of microcracks) and 397–405 °C (soot combustion on flat sides of a surface). The PEO coating on the titanium substrate showed a good adherence when subjected to an ultrasonic test, and improved after using weakly concentrated colloidal suspension for the formation of a thin TiO_2 layer.

© 2014 Elsevier B.V. All rights reserved.

1. Introduction

One of the main concerns for environmental protection is controlling the emission of soot particles from diesel engines and from toxic vehicular transport surges. Diesel exhaust particles consist mainly of highly agglomerated solid carbonaceous material, volatile organic and sulfur compounds, all of which result in adverse effects for human health. A promising technique of diesel exhaust abatement lies in the development of a catalytic filter, combining filtration and oxidation of the

emitted soot particulates. An uncatalyzed combustion of diesel soot occurs at 550–650 °C [1]. The temperature range of the exhaust gases of a diesel engine is 120–360 °C, and it is necessary to have active combustion catalysts within this temperature range to oxidize the soot. Many simple metal oxides, like CeO_2 , MoO_3 , V_2O_5 , CoO and CuO [1–3], and compositions combining transition metal oxides and alkaline or rare earth elements [4–9], were proposed for this purpose. However, among them it is possible to select only a few systems that meet rather strict requirements for catalytic coverings of the soot filters. Earlier we reported that CuMoO_4 efficiently catalyzes the combustion of soot from 340 °C with a significant increase of CO_2 selectivity [10]. Furthermore, its appreciable activity under loose contact conditions and high stability in the presence of SO_2 and water vapor demonstrated a favorable result for possible application of this catalyst in catalytic diesel filters [11].

Most of the research concerning the control of emissions of soot particles is executed on ceramic monoliths and foams [12–16]. However, the use of metals enables higher resistance of the diesel soot filters to both thermal and mechanical shocks [17]. The catalytic oxide compositions on a surface of metal should have a high activity for the soot oxidation, sufficient adherence, and thermochemical stability.

The combination of the plasma electrolytic oxidation technique (PEO) for the oxide film formation on titanium, and the impregnation technique by organic solution (extraction-pyrolytic method)

* Corresponding author at: Institute of Materials, Khabarovsk Scientific Centre, Far Eastern Branch of the Russian Academy of Sciences, 153 Tikhookeanskaya Street, Khabarovsk 680042, Russia. Tel.: +7 4212720888, +7 9243107078 (mobile); fax: +7 4212226598.

E-mail addresses: lnv1@yandex.ru (N.V. Lebukhova), rudnevvs@ich.dvo.ru (V.S. Rudnev), himicc@mail.ru (E.A. Kirichenko), pavel_ch@gorodok.net (P.G. Chigrin), lukiyanichuk@ich.dvo.ru (I.V. Lukiyanichuk), knf@mail.ru (N.F. Karpovich), pmaximal@mail.ru (M.A. Pugachevsky), kvg@ich.dvo.ru (V.G. Kurjavij).

¹ Tel.: +7 4212439886; fax: +7 4212226598.

² Tel.: +7 4232415208; fax: +7 4232312590.

³ Tel.: +7 9141646375; fax: +7 4212226598.

⁴ Tel.: +7 4212720888; fax: +7 4212 26598.

⁵ Tel.: +7 4232334456; fax: +7 4232312590.

⁶ Tel.: +7 9242073936.

⁷ Tel.: +7 9241081280; fax: +7 4232226598.

⁸ Tel.: +7 9024897578; fax: +7 4232312590.

or aqueous gel (sol–gel method) for support of catalytically active components was used [11]. Highly porous oxidic coatings produced by PEO method in silicate electrolyte greatly increase the surface area of the metal substrate improving the adherence of the catalyst layer. We have experimentally shown that the soot combustion start of the catalytic coating prepared by the extraction–pyrolytic method amounted to 270 °C, due to the presence of the CuMoO_4 grains with a fine size of up to 200 nm. In the case of the sol–gel method, the low activity of the catalyst revealed that might be associated with the formation on the oxidized titanium surface of the CuMoO_4 agglomerated crystals reaching the size of several microns. However, the aqueous gel has considerable ecological advantages in comparison with the extraction–pyrolytic technique, which uses volatile and very toxic organic reagents.

The influence of particle size and support–interactions on the redox behavior and catalytic properties is investigated for supported metal oxides [18]. The studies reveal that particle size and form of the metal oxide can be modulated by proper choice of the support. In a previous work we found that catalytic performance of the CuMoO_4 supported on the TiO_2 nanoparticles (50–70 nm) is considerably better in soot combustion than on SiO_2 nanoparticles (50–100 nm). The CuMoO_4 phase grains with diameter up to 50 nm were observed in the structure of the composition $\text{CuMoO}_4/\text{TiO}_2$ [19]. The aim of this research was to evaluate the effect of the nanostructural TiO_2 layer over the oxidized titanium surface on the structure of the CuMoO_4 catalytic coating, deposited using the sol–gel method, and its effects upon diesel soot combustion and stability.

2. Experimental section

2.1. Catalyst preparation

The oxide coatings were formed on the wires (\varnothing 1.2 mm) and plates ($25 \times 5 \times 1$ mm) of the titanium alloy VT1-0 (0.2 Fe, 0.1 Si, 0.07 C, 0.04 N, 0.12 O, 0.01 H and Ti > 99.6%) by PEO technique [20]. Prior to coating deposition, the substrates were stripped with emery buff and polished chemically in a mixture of concentrated acids (the volume ratio $\text{HF}:\text{HNO}_3 = 1:1$) at ~ 70 °C, followed by rinsing in distilled water and drying. The PEO treatment was conducted in aqueous electrolyte containing $0.05 \text{ mol} \cdot \text{l}^{-1} \text{Na}_2\text{SiO}_3$ and $0.16 \text{ mol} \cdot \text{l}^{-1} \text{NaOH}$. The PEO coating was formed on the titanium substrate being in an anodic polarization for 10 min at an average current density of $0.2 \text{ A} \cdot \text{cm}^{-2}$. The electrochemical cell consisted of a thermal glass with a spiral-shaped nickel cathode. The system was cooled by pumping cold water through the cathode to keep the electrolyte temperature below 35 °C. The final formation voltage was about 280 V. After anodic sparking treatment, the samples were rinsed with distilled water and air-dried at room temperature.

The TiO_2 layer was carried out using the TiO_2 colloidal suspension (22 wt.% anatase particles of 30–40 nm) prepared by solvothermal synthesis [21]. A mixture of toluene, oleic acid, and tetraisopropylate of titanium $\text{Ti}(\text{OC}_3\text{H}_7)_4$, as a precursor for TiO_2 , with a weight ratio of 10:5:1 was stored in the autoclave at a temperature of 250 °C for 24 h. The titanium wires and plates processed by the PEO technique were immersed into the TiO_2 colloidal suspension after 1 min. The samples were then calcined for 2 h in series at 120, 250, and 550 °C for successive steps in the evaporation of the solvents, pyrolysis of organic reagents, and carbon oxidation.

Polymeric gel was prepared by mixing water solutions of polyvinyl alcohol and salts of copper and molybdenum taken at molar ratios Cu:Mo 1:1. So, 1 M $\text{Cu}(\text{NO}_3)_2 \cdot 3\text{H}_2\text{O}$ solution in 0.2 M nitric acid and 0.1 M $(\text{NH}_4)_6\text{Mo}_7\text{O}_{24} \cdot 4\text{H}_2\text{O}$ solution in water were used. Previously 4.0 g of polyvinyl alcohol was individually dissolved in 40 ml of water and the solution was cooled at 5 °C. Then 17.8 ml of ammonium paramolybdate solution and 12.5 ml of copper nitrate solution were added consistently under magnetic stirring condition. Finally polymeric gel with total concentration of metals 2 wt.% was made by the addition

of water up to 100 g. The titanium wires structured by the PEO treatment and the TiO_2 layer were put for 30 min in the gel. The samples were then dried and heated in the air, at a temperature of 200 °C for 1 h, in order for the metals, salts and PVA to decompose, and then at 550 °C for 2 h for the oxidation of pyrolytic carbon and the formation of oxide phases.

2.2. Catalyst characterization

The phase composition of oxide coverings separated from a titanium substrate by mechanical method was determined by X-ray diffraction (XRD) using the D8 Advance Bruker diffractometer with CuK radiation. The phases were identified using Joint Committee on Powder Diffraction Standards (JCPDS) data. The morphology and structure of supported layers were investigated by Scanning Electron Microscopy (SEM) using the high-resolution microscope Hitachi S5500. The structure of nanoparticles was determined by Transmission Electronic Microscopy (TEM) with the LIBRA-120 ZEISS instrument. Specific surface area (BET) was defined by conventional N_2 adsorption at 77 K using a Sorbi 4.1 META apparatus. The coating adhesion was checked by the weight loss after treatment in an ultrasonic apparatus (frequency 40 kHz), with a generator power of 140 W.

2.3. Catalyst activity investigation

All experiments were performed using real diesel soot emitted by a torch flame from the combustion of diesel fuel; the BET surface area of diesel soot amounted to $62 \text{ m}^2/\text{g}$. The titanium wires with size of 10 mm were covered with soot emitted from a flame, a result of the combustion of diesel fuel up to an increase in the weight of the sample not less than 0.2–0.4 wt.%, for the realization of loose soot contact with the catalyst. The activity of the prepared catalyst toward soot combustion was analyzed in a dynamic gas atmosphere (50 ml/min), at a heating rate of 5 °C/min using thermo-analyzer STA 449 F3 NETZSCH. The catalytic test was carried out by gravimetric Thermal Analysis (TG) and Differential Thermal Analysis (DTA). The soot oxidation initiation temperature (T_i) was estimated from the intercept of a linear fit to the observed weight decrease with the zero line. The catalytic activity for the combustion of soot was determined as the temperature of maximum intensity (T_m) of exothermic DTA-curve.

3. Results and discussion

3.1. Catalyst compositions

The thickness of the coatings produced by the PEO treatment of titanium surface in silicate electrolyte reaches 10 μm . The elemental composition analysis of coatings showed presence (at.%) 70.9-O, 15.6-Si, 13.1-Ti and 0.4-Na. According to XRD of the oxide layer scraped off from a titanium substrate (Fig. 1a), the coatings include titanium oxide in structural modifications of rutile and anatase. None of the diffraction patterns show reflections from crystallized siliceous phases. According to previous investigation [22] silicon is present in the coating in the form of the amorphous silica. The typical surface of a titanium plate after PEO treatment (Fig. 2a) is rough: there are raised textures, hollows, and pores, which may be the traces of electric breakdowns or the outlets for gas bubbles. The oxide film consists of the crystallites with the size of 3–10 μm , and uniformly covers the surface of the titanium, with a pores diameter reaching 5–7 μm . The morphology of prepared composition $\text{CuMoO}_4/\text{TiO}_2 + \text{SiO}_2/\text{Ti}$ is demonstrated in Fig. 3. After impregnation with Cu and Mo and calcination at 550 °C the surface of the PEO coating is covered by agglomerated grains with size up to 10–12 μm . The elemental composition analysis of these particles determined a ratio of metals corresponding to the CuMoO_4 phase. The amount of supported catalyst was ~ 1.6 wt.%.

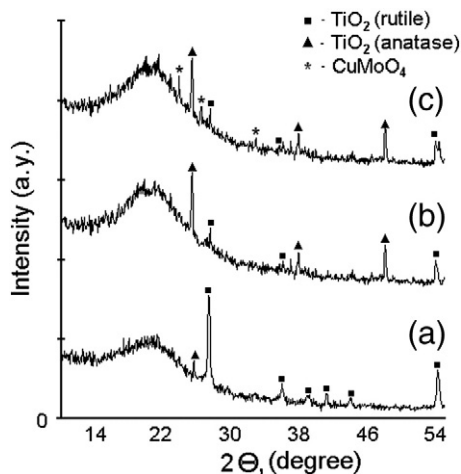


Fig. 1. XRD patterns of the oxide layers after (a) the PEO treatment of a Ti substrate, (b) after deposition of the TiO_2 layer, and (c) adding the active ingredients, Cu and Mo.

The average weight-growth of the oxidized titanium samples after immersion into the TiO_2 colloidal suspension and calcination treatment at a final temperature 550°C was 0.6–0.8 wt.%. The XRD pattern of the sample has shown the increase of the anatase structure diffraction peaks (Fig. 1b). The morphology of the structured support obtained at these temperatures is illustrated in Fig. 2b. The surface substrate is completely covered by a layer with an average thickness of 2–5 μm . The layer is divided by a grid of interconnected surface cracks with a width of 1–3 μm into separate monolith sites of 10–20 μm , on which ledges of fine-crystalline formations appear. According to the elemental local analysis, the covering consists of TiO_2 fine-crystalline formations on the surface. Silicon is also present (atomic ratio Si:Ti close to 1). Apparently, the colloidal suspension evenly fills micropores of the

substrate, and therefore after calcination treatment on the surface of the TiO_2 layer, the initial PEO coating appears. The formation of similar mosaic-type structures supported on an Al_2O_3 foam using colloidal suspension ZrO_2 has been described in report [14]. Observed surface cracks occur due to the shrinkage mechanism of the solvent evaporation process. We have experimentally confirmed that the cracking of the TiO_2 layer depends both on the pyrolysis temperature of the colloidal suspension organic part, and from a concentration of oxide particles. As shown in Fig. 2c the most intensive growth of cracks with a width of up to 3–7 μm occurs in pyrolysis temperature 350°C (final calcination temperature 550°C). Alternatively, a reduction in the quantity of cracks and their cross-section dimension up to 0.5–1.5 μm was observed using the suspension diluted by toluene three to five times (Fig. 2d). The morphology of the TiO_2 layer in more detail is illustrated in Fig. 4. The inside surface of the cracks possesses a highly-developed porous structure (Fig. 4a and b). Uniform structure of the monolith regions consists of particles of 30–50 nm connected among them (Fig. 4c). The electron diffraction pattern from the crystals located on a crack (in the inset to Fig. 2) corresponds to the structure of the anatase phase. The BET surface area of these samples amounted to $0.55\text{ m}^2/\text{g}$ ($0.01\text{--}0.02\text{ m}^2/\text{g}$ for the PEO coatings on titanium).

The XRD pattern of oxide composition after coating of the structured support by active ingredients, Cu and Mo, showed a presence of diffraction lines attributable to the CuMoO_4 triclinic structure (Fig. 1c). The amount of supported copper molybdate was ~0.5 wt.%. Fig. 5 demonstrates SEM images of the produced structured catalyst. The surface of nanostructural TiO_2 layer is evenly covered by roundish particles with a diameter of 150–350 nm. The results of elemental composition analysis indicate that there is nonhomogeneous allocation of the CuMoO_4 phase in different zones of the coating. A quantity of supported catalyst on the inside surface of the cracks (Cu—1.1 ÷ 1.7 at.%, Mo—1.0 ÷ 1.2 at.%, Ti—29.1 ÷ 27.5 at.%, oxygen, the balance) is sometimes below monolith regions (Cu—5.1 ÷ 7.6 at.%, Mo—5.2 ÷ 7.3 at.%, Ti—23.9 ÷ 21.3 at.%, oxygen, the balance).

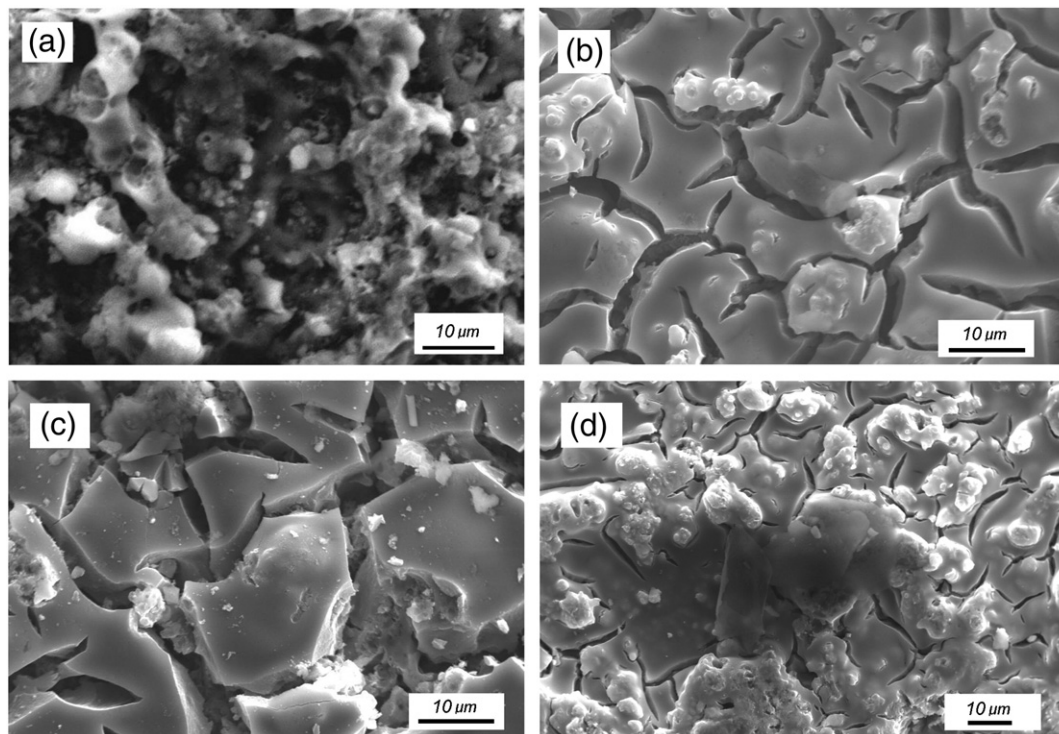


Fig. 2. SEM micrographs: (a) the PEO coating on a Ti substrate; (b)–(d) the TiO_2 layer after pyrolysis of initial colloidal suspension (b) at 350°C , (c) at 550°C , and (d) after pyrolysis at 350°C of colloidal suspension diluted by toluene three times.

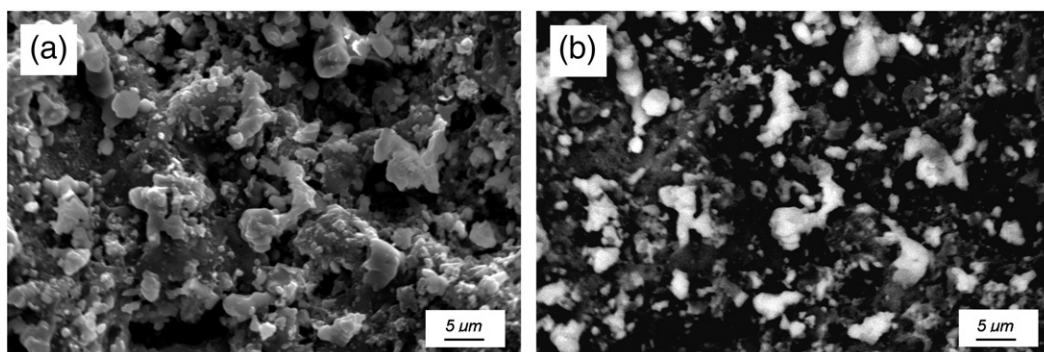


Fig. 3. SEM micrographs: (a) relief image and (b) phase image (lighter regions correspond to the CuMoO_4 phase) of the structured catalyst $\text{CuMoO}_4/\text{TiO}_2 + \text{SiO}_2/\text{Ti}$.

3.2. Catalytic soot combustion

The catalytic performance for diesel soot combustion of the supports ($\text{TiO}_2 + \text{SiO}_2/\text{Ti}$, $\text{TiO}_2/\text{TiO}_2 + \text{SiO}_2/\text{Ti}$) and the structured catalysts ($\text{CuMoO}_4/\text{TiO}_2 + \text{SiO}_2/\text{Ti}$ and $\text{CuMoO}_4/\text{TiO}_2/\text{TiO}_2 + \text{SiO}_2/\text{Ti}$) is presented in Fig. 6. The visible acceleration of soot conversion on TG-curves correlates to maximum DTA-curve exothermal effects, which allows identification of the registered loss of weight as soot combustion. The sample $\text{TiO}_2 + \text{SiO}_2/\text{Ti}$ provided a long temperature range of the soot oxidation from 420 °C up to 570 °C and the T_m value at 483 °C. The TG curve shape of the prepared compositions with the TiO_2 layer demonstrates two-stage soot combustion. Individual stages of the process are observed at initial temperatures of 340 and 460 °C for the structured support $\text{TiO}_2/\text{TiO}_2 + \text{SiO}_2/\text{Ti}$. The T_m values in the DTA profile of structured support $\text{TiO}_2/\text{TiO}_2 + \text{SiO}_2/\text{Ti}$ are located at 400 °C and 519 °C. After covering by the CuMoO_4 of the $\text{TiO}_2 + \text{SiO}_2/\text{Ti}$ surface the T_m value is reduced to 448 °C. The observed comparatively weak effect may be caused by a presence of large agglomerated crystals of the CuMoO_4 with sizes up to 10–12 μm (Fig. 3), as a result area of the surface

filled by the catalyst becomes less. The start of soot oxidation (T_i) significantly drops up to 280 °C, after a deposition of the CuMoO_4 catalyst on the surface of the TiO_2 layer. The DTA curves of this process represent a superposition of exotherms, with two visible extremums lying in the temperature ranges 340–362 °C and 397–405 °C. According to Neeft et al., similar double peaks on kinetic curves are explained by the presence of soot, which is in direct contact with a surface of the catalyst (tight contact), and with another part of soot removed from the catalyst (loose contact) [23]. However, the soot oxidation initial temperature of the structured catalyst $\text{CuMoO}_4/\text{TiO}_2/\text{TiO}_2 + \text{SiO}_2/\text{Ti}$ under loose contact conditions was much lower than previously tested bulk CuMoO_4 with particle sizes up to 3 μm (T_i –330 °C, T_m –387 °C) under tight contact conditions. The activity of the structured catalyst agrees with similar results reported in our previous work for the CuMoO_4 grains, with a diameter up to 200 nm, in the structure of compositions $\text{CuMoO}_4/\text{TiO}_2 + \text{SiO}_2/\text{Ti}$ produced by the extraction-pyrolytic technique [11]. The influence of particle size of mixed metal oxides and structured catalysts on their activity for soot combustion was considered in some reports [24,25]. In the fine-grained phase, the surface area, the reactivity

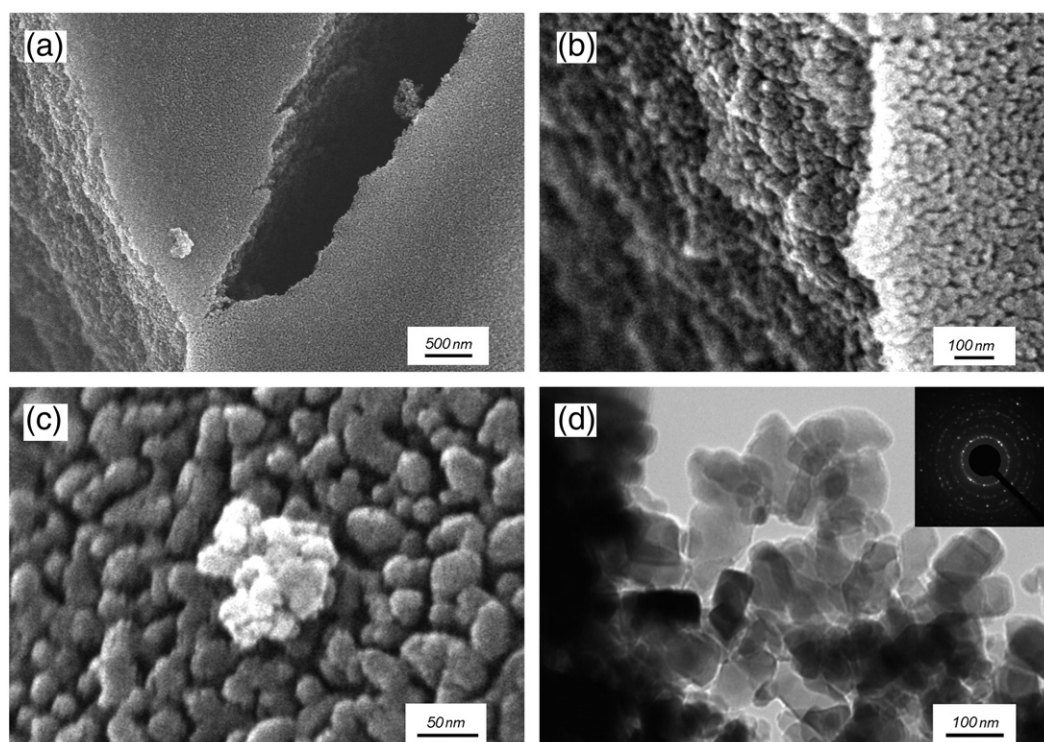


Fig. 4. SEM micrographs of the TiO_2 layer (a–c) with different magnifications and (d) TEM image of the crystals located on a crack (in the inset the electron diffraction pattern).

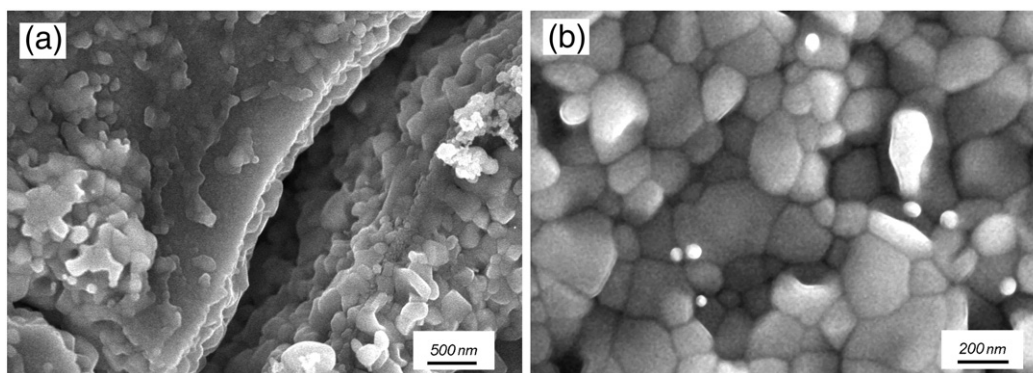


Fig. 5. SEM micrographs of the structured catalysts $\text{CuMoO}_4/\text{TiO}_2/\text{TiO}_2 + \text{SiO}_2/\text{Ti}$ (a, b with different magnifications).

and the concentration of active sites of catalyst greatly increase. Thus, they show drastically improved catalytic properties.

Earlier we showed that high catalytic activity CuMoO_4 is caused by redox interaction between the particle surface of the copper molybdate and soot [10]. The reduction of copper ions is accompanied by the formation of an active $\text{Cu}_4 - x\text{Mo}_3\text{O}_{12}$ phase, where catalytic reaction occurs. This gives some grounds to conclude that lowering the value T_i of soot combustion of both structured catalysts is associated with high reactivity of the CuMoO_4 phase grains with a diameter up to 200–350 nm. According to experimental data, there is a difference in intensity in the initial stages of the kinetic curves of the catalysts obtained using the substrates with different microstructures of the TiO_2 layer (Fig. 2b, c, and d). The magnitude of the DTA effect consistently drops with a reduction in the quantity and width of cracks. Apparently, the initial stage is caused by the combustion of soot contained in the spaces of the cracks. Visible rate maximums at a temperature interval of 280–370 °C arise due to a high reaction exothermicity, and local heat inside the cracks. The developed, highly porous structure inside the surface of the cracks also can influence the supported catalyst activity.

3.3. Coating mechanical stability

To test the adherence of the coatings obtained on the titanium substrate, the samples were immersed in water and subjected to ultrasound for differing durations. Subsequently, the samples were dried at 110 °C and weighed. Banús et al. have recently applied this kind of analysis for ZrO_2 layers on ceramic support [14] and Cebollada et al. for adherence testing of alumina coating over stainless steel [26]. Fig. 7 shows the weight loss of the samples after an ultrasonic treatment in water for 30 min. The PEO coating on the titanium substrate showed good adherence when subjected to an ultrasonic test. A low stability is determined for the structured catalyst $\text{CuMoO}_4/\text{TiO}_2/\text{TiO}_2 + \text{SiO}_2/\text{Ti}$. After an ultrasonic treatment for 10 min, more than 60 wt.% of the TiO_2 layer was removed. Mechanical stresses can result in both the peeling of the coating and destruction within the coating. The SEM-image of the sample after ultrasonic treatment (Fig. 8) demonstrates only a cohesive failure of the TiO_2 layer. According to the elemental composition analysis, the major destruction occurs in the locations of surface microcracks of the TiO_2 layer. Components of the supported catalyst are detected on nonfailed flat areas of the layer. The elemental composition of the surface at places of augmented microcracks was comparable with initial TiO_2 layer. Probably, the mechanism of cohesive failure is associated with a stress concentration near the borders of microcracks caused by shrinkage of the layer during a drying process.

A good adhesion of the layer can be explained by the high porosity of the oxidized titanium surface. The mechanical stability of the structured catalyst was improved using a colloidal suspension diluted by toluene three times to form the TiO_2 layer. Apparently, the excellent mechanical stability of this sample is associated with the decrease in internal stresses of a thin layer of TiO_2 . After ultrasonic treatment, surface damage of the catalyst and a reduction of its soot combustion activity were not observed.

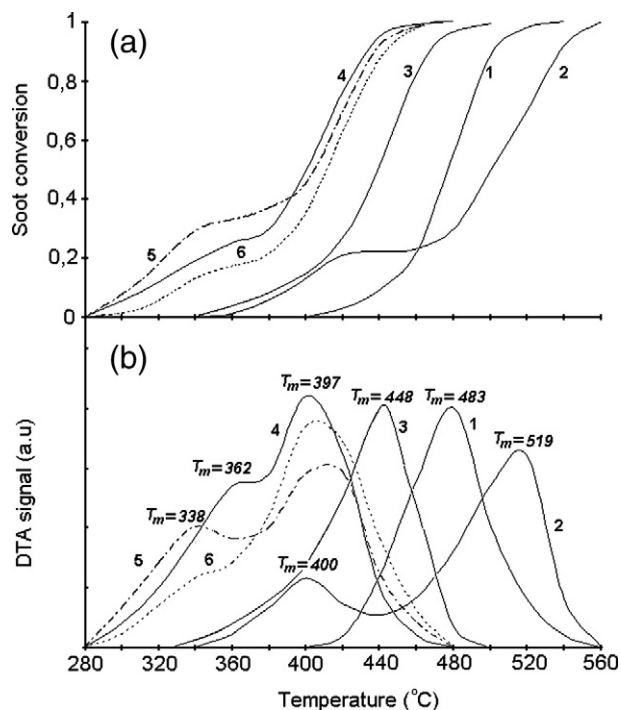


Fig. 6. TG (a) and DSC (b) curves of diesel soot combustion of the structured system (1) $\text{TiO}_2 + \text{SiO}_2/\text{Ti}$, (2) $\text{TiO}_2/\text{TiO}_2 + \text{SiO}_2/\text{Ti}$, (3) $\text{CuMoO}_4/\text{TiO}_2 + \text{SiO}_2/\text{Ti}$, $\text{CuMoO}_4/\text{TiO}_2/\text{TiO}_2 + \text{SiO}_2/\text{Ti}$ with different TiO_2 layer microstructures, (4) after pyrolysis of initial colloidal suspension at 350 °C, (5) at 550 °C and (6) after pyrolysis at 350 °C of colloidal suspension diluted by toluene three times.

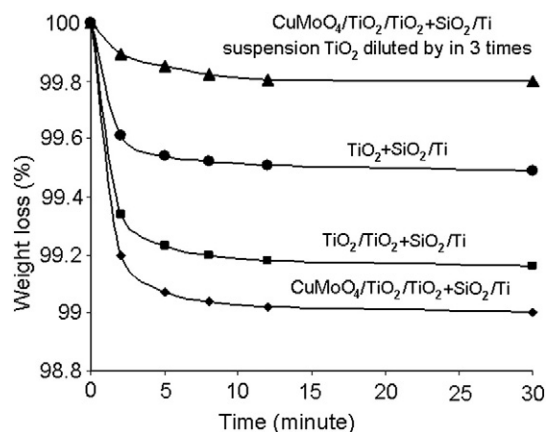


Fig. 7. Mechanical stability test (ultrasonic bath with water) of the structured systems.

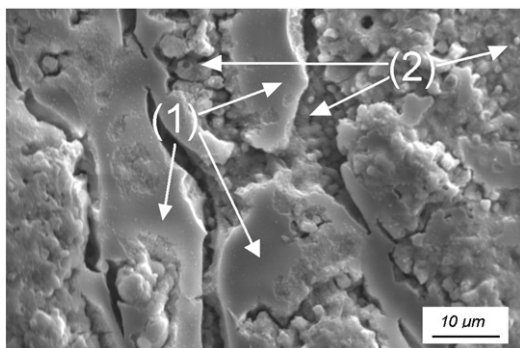


Fig. 8. SEM micrograph of the TiO₂ layer (pyrolysis of initial colloidal suspension at 350 °C) after ultrasonic treatment for 10 min: (1) nonfailed flat areas, (2) cohesive failure of microcracks.

4. Conclusion

The structural catalyst CuMoO₄/TiO₂/TiO₂ + SiO₂/Ti for diesel soot combustion was made using a sequential process. After PEO treatment, the oxide film uniformly covering a titanium surface consists of the crystallites with a size of 3–10 μm; and the diameter of the pores reached 5–7 μm. The elemental composition analysis of coatings showed a presence (at.%) of 15.6-Si and 13.1-Ti. After impregnation with the TiO₂ colloidal suspension and calcination treatment at a final temperature 550 °C, the PEO coating surface was completely covered by a layer with an average thickness of 2–5 μm, which consists of the cubic form anatase crystals with ribs up to 50 nm. The TiO₂ layer morphology presents a mosaic-like structure with interconnected surface microcracks. The cracking of the TiO₂ layer depends upon both the pyrolysis temperature of the colloidal suspension organic part, and a concentration of oxide particles. The CuMoO₄ catalytic coating deposited on the TiO₂ layer is generated by particles of 150–350 nm, which can explain the high reactivity of the structural catalyst under loose contact conditions. The structured catalysts CuMoO₄/TiO₂/TiO₂ + SiO₂/Ti

provide diesel soot combustion above 280 °C, with a maximum of two at the rate at 340–360 °C (soot combustion in volume of microcracks) and 397–405 °C (soot combustion on flat sides of a surface). After ultrasonic treatment, a cohesive failure of this layer only was observed. The mechanical stability of the structured catalyst was improved using a colloidal suspension diluted by toluene three times, for the formation of a thinner layer of TiO₂.

References

- [1] B.R. Stanmore, J.F. Brilhas, P. Gilot, *Carbon* 39 (2001) 2247–2268.
- [2] J.P.A. Neeft, M. Makkee, J.A. Moulijn, *Appl. Catal. B Environ.* 8 (1996) 57–78.
- [3] K. Shimizu, H. Kawachi, A. Satsuma, *Appl. Catal. B Environ.* 91 (2009) 489–498.
- [4] G. Neri, G. Rizzo, S. Galvagno, A. Donato, M.G. Musolinob, R. Pietropaolo, *React. Kinet. Catal. Lett.* 78 (2003) 243–250.
- [5] K. Krishna, A. Bueno-López, M. Makkee, J.A. Moulijn, *Appl. Catal. B Environ.* 75 (2007) 189–200.
- [6] H. An, C. Kilroy, P.J. McGinn, *Catal. Today* 98 (2004) 423–429.
- [7] C. Gong, Ch. Song, Y. Pei, G. Lv, G. Fan, *Ind. Eng. Chem. Res.* 47 (2008) 4374–4378.
- [8] M.A. Hasan, M.I. Zaki, K. Kumari, L. Pasupulety, *Thermochim. Acta* 320 (1998) 23–32.
- [9] V.G. Milt, C.A. Querini, E.E. Miró, *Thermochim. Acta* 404 (2003) 177–186.
- [10] P.G. Chigrin, N.V. Lebukhova, A.Yu. Ustinov, *Kinet. Catal.* 54 (2013) 76–80.
- [11] N.V. Lebukhova, V.S. Rudnev, P.G. Chigrin, I.V. Lukiyanichuk, M.A. Pugachevsky, A.Ju. Ustinov, E.A. Kirichenko, T.P. Yarovaya, *Surf. Coat. Technol.* 231 (2013) 144–148.
- [12] D. Fino, P. Fino, G. Saracco, V. Specchia, *Chem. Eng. Sci.* 58 (2003) 951–958.
- [13] D. Fino, *Sci. Technol. Adv. Mater.* 8 (2007) 93–100.
- [14] E.D. Banús, V.G. Milt, E.E. Miró, M.A. Ulla, *Appl. Catal. A Gen.* 362 (2009) 129–138.
- [15] E.D. Banús, V.G. Milt, E.E. Miró, M.A. Ulla, *Appl. Catal. B Environ.* 132–133 (2013) 479–486.
- [16] L. Sui, L. Yu, *Chem. Eng. J.* 155 (2009) 508–513.
- [17] B.A.A.L. van Setten, M. Makkee, J.A. Moulijn, *Catal. Rev. Sci. Eng.* 43 (2001) 489–564.
- [18] D. Srinivas, P. Ratnasamy, in: B. Zhou, S. Han, R. Raja, G.A. Somorjai (Eds.), *Nanotechnology in Catalysis*, V. 3, Springer Science + Business Media, LLC, New York, 2007, p. 183.
- [19] N.V. Lebukhova, N.F. Karpovich, E.A. Kirichenko, K.S. Makarevich, M.A. Pugachevsky, *Vopr. Materialovedeniya* 1 (2013) 88–94.
- [20] V.S. Rudnev, *Surf. Coat. Technol.* 235 (2013) 134–143.
- [21] X. Chen, S.S. Mao, *Chem. Rev.* 107 (2007) 2891–2959.
- [22] Y.M. Wang, T.Q. Lei, L.X. Guo, B.L. Jiang, *Surf. Coat. Technol.* 201 (2006) 82–89.
- [23] J.P.A. Neeft, O.P.Y. Pruijsen, M. Makkee, J.A. Moulijn, *Appl. Catal. B Environ.* 12 (1997) 21–31.
- [24] C.N. Chervin, B.J. Clapsaddle, H.W. Chiu, A.E. Gash, J.H. Satcher Jr., S.M. Kauzlarich, *Chem. Mater.* 18 (2006) 1928–1937.
- [25] K.N. Rao, P. Venkataswamy, B.M. Reddy, *Ind. Eng. Chem. Res.* 50 (2011) 11960–11969.
- [26] P.A.R. Cebollada, E. Garcia-Bordejé, *Chem. Eng. J.* 149 (2009) 447–454.